Robotica (2015) volume 33, pp. 933–952. © Cambridge University Press 2014
doi:10.1017/S0263574714000691

Optimal regulation of a cable robot in presence of obstacle using optimal adaptive feedback linearization approach

M. H. Korayem*, H. Tourajizadeh, A. Zehfroosh and A. H. Korayem

Robotics Research Laboratory, Center of Excellence in Experimental Solid Mechanics and Dynamics, School of Mechanical Engineering, Iran University of Science and Technology, Tehran, Iran

(Accepted February 19, 2014. First published online: March 21, 2014)

SUMMARY

Optimal path planning of a closed loop cable robot, between two predefined points in presence of obstacles is the goal of this paper. This target is met by proposing a new method of optimal regulation for non linear systems while Dynamic Load Carrying Capacity (DLCC) of the robot is supposed as the related cost function. Feedback linearization is used to linearize the system while Linear Quadratic Regulator (LQR) is employed to optimize the DLCC of the system based on torque and error constraints. Obstacle avoidance for both the end-effector and cables is also considered by the aid of designing an adaptive local obstacle avoidance controller. As a result of linearized nature of the proposed optimal regulation and obstacle avoidance, fast calculation for real time applications is possible. Therefore, formulation of the optimal feedback linearization, together with calculating the DLCC of the robot based on the presented constraints is derived. Finally, a simulation study is performed to study the optimal dynamics and also the maximum DLCC of the cable robot in presence of obstacles. Simulation results are eventually compared with experimental tests conducted on IUST Cable Suspended Robot (ICaSbot) to verify the validity and efficiency of the proposed optimal controllers.

KEYWORDS: Cable suspended robot; Feedback linearization; Optimal regulation; Dynamic load capacity; Adaptive local obstacle avoidance.

1. Introduction

Cable robots are considered as a modified version of cranes, aiming to handle objects with better control. Any kind of disturbing oscillations and swings can be damped using proper controlling signals. Therefore, optimizing the payload of the robot as the most important parameter cable robots can be a useful study for different applications such as object handling in industrial environments, rehabilitation, cranes, etc. Moreover, ordinary cranes are not capable of supporting the objects movement in all spatial directions while designed cable robots have the advantage of providing all six spatial Degrees of Freedom (DOFs) for an object in the space. In addition, common traditional cranes cannot be used in environments that include obstacles. Since the dynamic workspace of cable robots is so large, the end-effector usually faces lots of obstacles which should be bypassed using a proper obstacle avoidance strategy. Based on these expectations, a proper optimal closed loop controlling method is required for cable robots to carry the maximum payload along with satisfying the obstacle avoidance condition at the same time. The method should be local to bypass the obstacle in an on-line way and it should be fast enough to be useful for real-time applications as well.

* Corresponding author. E-mail: hkorayem@iust.ac.ir

Some researches have been performed in this area so far. Iterative Linear Programming method is employed by ref. [1] for a cable robot in order to maximize the payload while Hamilton-Jacobi-Bellman method is used for the same robot and the same cost function in ref. [2]. Since these cases are open loop, any kind of disturbances or parametric uncertainties ruins the desired results. Besides, some point to point path planning of the robots has to be performed globally and in off-line way which is not suitable for on-line application. For example, Particle Swarm Optimization which is employed in ref. [3] is related to this category. To prevent from these disorders, closed loop methodologies are employed in some literatures. Feedback linearization is used for optimal distribution of cables tension for a constrained sample of a cable robot in ref. [4] by Spong. Gholami *et al.*[5] optimized a constrained sample of cable robot in order to achieve minimum cables tension. State-Dependent Riccati Equation is used in ref. [6] to optimal control of a flexible cable transporter system while the stability is guaranteed by robust H-infinity method. Most of these researches also suffer from two main disadvantages. First of all the optimization process requires a huge mathematical calculation as a result of their non linear objective functions which decreases the rate of on-line process and limits their experimental applications. Secondly, an important constraint, i.e., obstacle avoidance is ignored in these researches. Again obstacle avoidance problem which is considered in many literatures either uses offline procedures or local but with a nonlinear objective function. Open loop path planning of a mobile robot in presence of obstacle is discussed by Korayem *et al.*[7] which is not robust against disturbances. Potential field method that is employed in ref. [8] and potential function of ref. [9] for bypassing the obstacles needs nonlinear objective function and thus high calculation procedure is required which is not suitable for real-time processes. In cell decomposition and roadmap[10] which are employed in the literatures, the path should be planned globally or in an off-line way which is not suitable for online application. Local method of Bug algorithm and path searching by local planning which are used in ref. [11] also do not necessarily guarantee the optimality of the produced path. Moreover, obstacle avoidance for cable robots has not been studied yet except for cranes. Forest[12] planed a path for a crane to optimize the motors torque in presence of obstacle. Input shaping is used to control the load in this research. But these cranes are not capable of supporting all of DOFs of the load.

It can be seen that in most of previous algorithms, the objective function remains nonlinear, so a nonlinear optimization process is required which results in either offline path planning or online one with huge mathematical calculations that are not applicable in real time procedures. So in this paper a real time methodology is proposed for the cable robot in order to plan the optimal path in an on-line way using a new method of optimal regulation of nonlinear systems subject to its DLCC while the local obstacles can be bypassed simultaneously and in an online way. Optimal feedback linearization method along with LQR is used here to cover the mentioned targets and improve the explained deficiencies. The advantage of the proposed optimization algorithm is that the destructive effects of disturbances, uncertainties, and also the risk of obstacle collision are canceled since the optimization and path planning is performed in a closed loop way. Feedback linearization provides exact linearization throughout the workspace of the robot and guaranties Lyapunov stability. In addition, LQR ensures the optimization with an acceptable phase and gain margins. Moreover, combination of feedback linearization with LQR makes it possible to analytically optimize a non linear system in a closed loop way with a fast calculation process in an on line way which can be easily and practically implemented in experimental manipulations during real time operations. Finally, a novel method of adaptive obstacle avoidance in optimal regulation is proposed. Any kind of stationary or moving obstacles in any environmental situation can be locally bypassed in an online way using the proposed algorithm while the optimality of the path is guaranteed and its linearized nature makes it possible to be fast and applicable for real time applications. By the aid of proposed algorithm not only can the obstacle be bypassed by the end-effector but also collision between the obstacle and the cables can be avoided. Thus, online and closed loop optimal path planning is provided here together with local and adaptive obstacle avoidance with a fast mathematical real time operation as a result of using a linear objective function for nonlinear complicated dynamics of cable robot plants.

To meet this goal, the related state space of the system is linearized using feedback linearization method then, LQR can be used to optimize the controller gains of the closed loop system subject to DLCC cost function. Required motors torque and tracking error between two predefined points are the main constraints in defining the DLCC. Collision between end-effector and cables with stationary and moving obstacles is also avoided locally by defining a new set point and adding an adaptive

https://doi.org/10.1017/S0263574714000691 Published online by Cambridge University Press

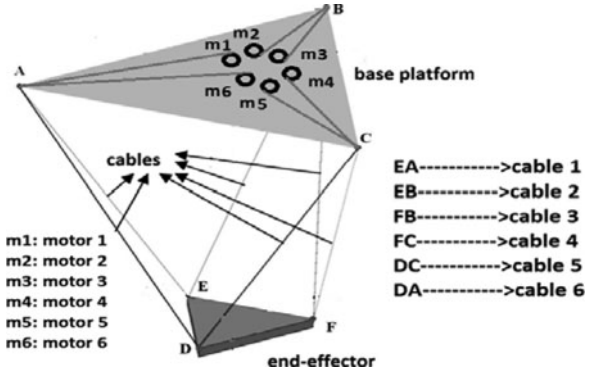

Fig. 1. A scheme of cable robot with six cables.

obstacle avoidance controller to the designed controller. The efficiency of the designed controller is verified by the aid of some simulations. The optimal path is obtained and also obstacle avoidance is verified by positioning both of stationary and moving obstacles in different locations within the way of the obtained optimal path of the end-effector and cables. Afterward, maximum DLCC of the closed loop cable robot is calculated. Simulation results are finally compared with experimental tests conducted on ICaSbot which is an under constrained cable robot with six DOFs and six suspending cables. Not only the validity of the optimal regulation process is shown, but also the efficiency of the proposed obstacle avoidance controller is proved.

2. Control Scheme

2.1. Optimal feedback linearization control strategy

For an under constrained spatial cable robot with six DOFs and six supporting cables as Fig. 1, dynamic equation of the end-effector can be described by Eq. (1):[13]

$$D(X)\ddot{X} + C(X, \dot{X})\dot{X} + \hat{g}(X) = -S_J^T(q(X))T; \quad X = \{x_m, y_m, z_m, \psi, \Theta, j\}, \tag{1}$$

where X is a 6 DOF pose vector including the three translations x,y,z and the three rotations ψ, Θ, φ. D is the inertia matrix of the robot, C is its Coriolis matrix, $\hat{g}$ is the vector of gravity, S_J is the Jacobian matrix of the robot:

$$D = \begin{bmatrix} mI_3 & 0 \\ 0 & P^T I P \end{bmatrix}; C = \begin{bmatrix} 0_3 \\ P^T\{I\dot{P}\dot{o} + (P\dot{o}) \times I(Po)\} \end{bmatrix}; \hat{g} = \begin{bmatrix} 0 \\ 0 \\ -mg \\ 0_3 \end{bmatrix}; S_J = \left[\frac{\partial q_i}{\partial x_j}\right]_{i\times j};$$

$$P = \begin{bmatrix} 1 & 0 & -\sin\theta \\ 0 & \cos\psi & \sin\psi\cos\theta \\ 0 & -\sin\psi & \cos\psi\cos\theta \end{bmatrix}; \dot{o} = \begin{bmatrix} \dot{\Psi} \\ \dot{\theta} \\ \dot{\varphi} \end{bmatrix}.$$

T is the vector of cables tension, X is the task space vector of DOFs of the end-effector, m and I are the mass and moment of inertia of the end-effector and q is the length of the cables.

Considering motor dynamics, the following feed forward motors torque can be concluded:[13]

$$\tau = rT + J\ddot{\beta} + C_v\dot{\beta}; \quad T = \{S_J^{-T}(D(X)\ddot{X} + C(X, \dot{X}) + g(X))\}, \tag{2}$$

where r is the diagonal matrix of drum radius, T is the required feed forward vector of cable tension (since it is calculated using the inverse dynamics of the system based on the desired path and will be improved by adding feedback terms in the proposed optimal control in the next section), J is the diagonal matrix of rotary inertia of the motors, C_v is the diagonal matrix of the viscous friction of the

https://doi.org/10.1017/S0263574714000691 Published online by Cambridge University Press

motors (the friction of the cable transmission is neglected since it is negligible compared to the motor viscous friction), $\dot{\beta}$ is the vector of angular velocity of the motors and τ is the vector of motors torque. In order to achieve the highest DLCC, the error and input should be optimized here, by using LQR. Thus, it is first necessary to linearize the state space by employing an exact method like feedback linearization. It was shown in ref. [14] that based on feedback linearization, following torque vector transfers the state space of the system to a linearized one:

$$\tau = rS_J^{-T}(D\nu + C + g) + J\ddot{\beta} + C_v\dot{\beta}; \quad \nu = \ddot{X}_d + u; \quad u = K_p e + K_d\dot{e} + K_i \int e, \tag{3}$$

where ν is the controlling input vector of the linearized state space of the system, u is the PID terms of this input, for which its gains should be optimized by using LQR, $\ddot{X}_d$ is the desired acceleration vector of the DOFs, e is the vector of DOFs error and K_p,K_d,K_i are the controlling gains of position error, velocity error, and integral of error respectively. Based on the linearized state space of the system, controlling input of the linearized system (u) can be optimized by the aid of LQR in order to optimize the DLCC.[14] Since time is not considered as the constraint terms of optimization process of DLCC [22], the objective function can be defined as ref. [15]:

$$J(X) = \int_{t_0}^{\infty} (e_r(X,t)^T Q e_r(X,t) + u(X,t)^T R u(X,t))dt; \quad e_r = [e;\dot{e}], \tag{4}$$

where Q and R are positive definite matrices of accuracy and input gains and e_r is the error vector of state space (including the DOFs error and their relative derivatives). Solving the Riccati equation related to the above objective function based on LQR method results in the following optimal controlling input:[15]

$$u^* = -R^{-1}B^T S e_r(X,t), \tag{5}$$

where u^* is the optimal input vector of linearized system, B is the input matrix of the state space of the robot system, and S is the resultant matrix of solving the mentioned Riccati equation.[15] Substituting this optimal input in Eq. (3) results in the following controlling torque:

$$\tau = rS_J^{-T}(D(\ddot{X}_d - R^{-1}B^T S e_r(X,t)) + C + g) + J\ddot{\beta} + C_v\dot{\beta}. \tag{6}$$

Overall scheme of the proposed optimal feedback linearization control in presence of obstacle can be seen in Fig. 3. Internal closed loop of the motor is controlled each 0.01 sec while outer closed loop of the end-effector is controlled each 0.1 s. These sample rates are the best choices for the studied robot which are estimated experimentally according to the dynamic time constant specifications of the motors and the end-effector during their sequential controlling process. That's why an obstacle avoidance strategy is required with a fast calculation capability which could be implemented experimentally and in an on-line way with the mentioned controlling time step. The optimal path can be achieved analytically and in an on-line way by solving the following differential equation:

$$\ddot{X} = \frac{1}{D(X)}(-C(X,\dot{X})\dot{X} - g(X) + S_J(\{S_J^{-T}(D(X)(\ddot{X}_d + u*) + C(X,\dot{X}) + g(X))\})). \tag{7}$$

2.2. Obstacle avoidance strategy

The main duty of the designed cable robot is load handling between two predefined points in an industrial environment and this kind of places are usually full of equipments which play the role of obstacles for the robot. Therefore, one feature that should be considered while designing the controller is the obstacle avoidance capability for both the end-effector and cables. It is desired here that the end-effector tracks the nearest path to the optimal one at the same time with satisfying the obstacle avoidance condition. So to bypass the local obstacles and also avoid the nonlinearity in the objective function which increases the speed of process for on-line applications, it is proposed here to define a

https://doi.org/10.1017/S0263574714000691 Published online by Cambridge University Press

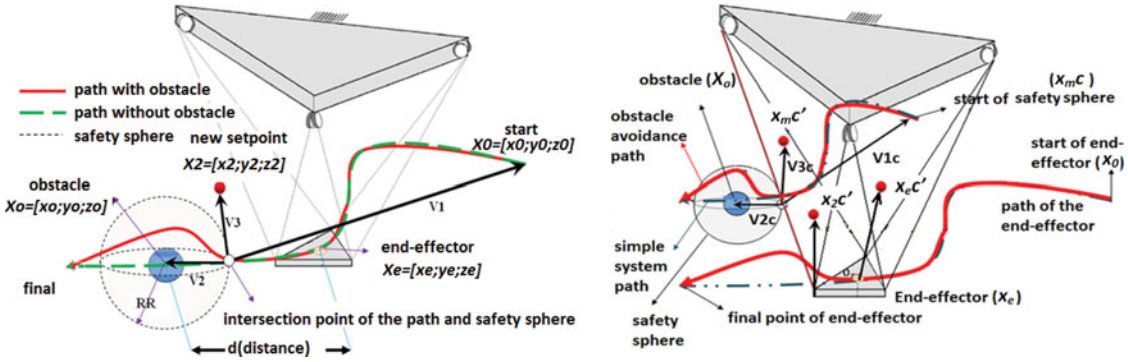

Fig. 2. The procedure of defining the new set point of end-effector in order to bypass the obstacles (left), The procedure of defining the new set point of cable' risky point in order to bypass the obstacles (right).

new setpoint and new objective function as Eq. (10).[7] A critical zone is defined around the obstacle by a safety sphere with radius (*RR*) in where an extra controlling signal affects on the end-effector as soon as entering the end-effector into the mentioned critical zone. The obstacle with every geometrical configuration is supposed to be a sphere with radius (r_o) which encompasses the obstacle and this assumption increases the reliability of the obstacle avoidance. Also since the obstacle avoidance is provided between the obstacle and the sphere which encompasses the end-effector, the rotation of the end-effector does not make any change in the solution and it provides a higher margin of safety for us.

This extra controlling command is produced by defining a new set point for the end-effector during the presence of the end-effector within the critical zone. By the other word, however the end-effector is a triangle, in this paper in order to satisfy a higher level of safety, the circumscribed sphere to the end-effector triangle is supposed as the TCP (Tool Center Point) which should be avoided of being collided with the obstacle and this importance is realized using the proposed method. Based this algorithm of this paper, this local obstacle can be placed in every environmental situation in the way of end-effector or cables and it can be also either stationary or moving. To meet this goal two vectors are defined. The cross product vector of these two vectors produces a vector perpendicular to the plane of these two vectors which tends to push the end-effector tangent to the sphere around the obstacle. The radius of this sphere is defined based on required safety distance. This obstacle avoidance control signal is optimal since it is calculated using the same objective function of Eq. (10). Since LQR is a an analytic tool of optimization, the obtained control input for the outer closed loop of feedback linearization is necessarily optimum considering the mentioned objective function. It is desired for us that the robot bypass the obstacle in a way that the minimum divergence would be occur respect to the obtained optimal path which was extracted for the case in which there is no obstacle engaged in (the more divergence, the more violence in the optimality and the more required controlling input). So it bypasses the obstacle with the nearest path respect to the optimal one. Moreover, contrary to potential field method, the objective function remains linear since minimizing a distance respect to a new setpoint is considered in the objective function rather than maximizing the distance respect to the obstacle. This linearity makes it possible to be used in fast analytic optimization tool of LQR. This procedure can be seen in Fig. 2(left). The two mentioned vectors can be defined as:

$$V3 = V1 \times V2; \quad V1 = [x0 - xe; y0 - ye; z0 - ze]^T, \quad V2 = [xo - xe; yo - ye; zo - ze]^T, \tag{8}$$

where X_0 is the vector of initial point of the end-effector movement and X_O is the position vector of the obstacle. So the new set point can be defined:

$$X_{2e} = X_e + \alpha(d).(V3/\|V3\|), \tag{9}$$

https://doi.org/10.1017/S0263574714000691 Published online by Cambridge University Press

where X_{2e} is the vector of new set point related to obstacle avoidance, X_e is the position vector of the end-effector, $\alpha(d)$ is a gain which is a function of distance between the obstacle and the end-effector (d). Therefore, a pair of objective functions is defined here for these two set points:

$$J_1(x) = \int_{t_0}^{\infty} (e_r(X,t)^T Q e_r(X,t) + u_1^T R u_1) dt; \quad J_2(x) = \int_{t_0}^{\infty} (e_{r2}(X,t)^T Q_o e_{r2}(X,t) + u_2^T R_o u_2) dt, \tag{10}$$

where $e_r(X,t)$ is the distance and its derivative vector between the end-effector and the main set point which is the final desired point of the end-effector, $e_{r2}(X,t)$ is the same variable between the end-effector and the temporary set point which is the desired point related to obstacle avoidance controller (X_2), u_1 and u_2 are controlling input vectors of linearized system related to the main setpoint and obstacle avoidance setpoint respectively and Q_o and R_o are accuracy and input gains of obstacle avoidance movement.

Based on these two objective functions, two optimal controlling signals can be produced (u_{1^*} and u_{2^*}). Since in a regulation process $\ddot{X}_d$ is zero, based on Eq. (3) we have:

$$u_{1^*} = v_e = -R^{-1} B^T S_{e_r}(X,t); \quad u_{2^*} = v_o = -R_o^{-1} B^T S e_{r2}(X,t), \tag{11}$$

where, v_e and v_o are optimal controlling input vectors of feedback linearization for the main set point and obstacle avoidance setpoint, respectively. The final control signal vector is u_{1^*} if the end-effector is out of critical zone while it will be the summation of these two command vectors ($u_{1^*}+u_{2^*}$) if the distance of the end-effector to the obstacle is less than a predefined allowable value RR of safety sphere. This summation helps the end-effector bypass the obstacle and approach to the main setpoint simultaneously. Of course, this strategy like other ones provides an acceptable convergence to the setpoint if there would be an acceptable distance between the final setpoint and the location of the obstacle. However, in order to provide the adaptivity of the obstacle avoidance respect to the environmental position and velocity of the obstacle, each of the mentioned controlling signals are multiplied by some adaptive controlling gains which causes the end-effector bypass the obstacle in every position and with any velocity with a roughly same amplitude of motor torque. The final optimal path in presence of obstacle can be again determined based on Eqs. (7) for which the optimal controlling term of u^* is substituted by this calculated controlling term of Eq. (11). Considering the fact that the same strategy of analytic LQR based optimization is also employed for obstacle avoidance, it can be concluded that for both cases, the gained path is optimal for the outer closed loop part of controlling signal.

The obstacle can be also placed along the path of a cable, or several cables of the robot. The same proposed procedure can be implemented for avoiding the collision between the obstacle and each cable (Fig. 2(right)). For this purpose, it is first required to find out the perpendicular projection of the obstacle along the risky cable i ($X_m c_i$):

$$X_m c_i = X_1 c_i + \sum_{j=1}^{3}((-(X_2 c_i(j) - X_1 c_i(j))(X_1 c_i(j) - X_o(j))/\sum_{j=1}^{3}(X_2 c_i(j) - X_1 c_i(j))^2 (X_2 c_i(j) - X_1 c_i(j)); \quad i = 1, ..6, \tag{12}$$

where $X_1 c_i$ and $X_2 c_i$ are the coordinates of the two end sides of the risky cable line i, respectively. The mentioned vectors in previous section can be defined for this projection point:

$$\left.\begin{aligned} V_1 c_i &= [X_o(1) - X_m c_i(1); X_o(2) - X_m c_i(2); X_o(3) - X_m c_i(3)] \\ V_2 c_i &= [X_1 c_i(1) - X_m c_i(1); X_1 c_i(2) - X_m c_i(2); X_1 c_i(3) - X_m c_i(3)] \end{aligned}\right\}$$
$$\Rightarrow V_3 c_i = V_1 c_i \times V_2 c_i; \quad i = 1, ..6. \tag{13}$$

https://doi.org/10.1017/S0263574714000691 Published online by Cambridge University Press

So it is possible to define the new obstacle avoidance set point for the projection point of the cable ($X_m c_i'$):

$$X_m c_i' = X_m c_i + \alpha_c(d)(V_3 c_i / \| V_3 c_i \|), \tag{14}$$

where $\alpha_c(d)$ is the gain of the setpoint as a function of the distance between the projection point and obstacle. Based on the new setpoint of the projection point it is possible to find out the new setpoint of the second point of the cable ($X_2 c_i'$):

$$X_2 c_i' = X_2 c_i + ((X_m c_i' - X_m c_i)(X_2 c_i - X_1 c_i)/(X_m c_i - X_1 c_i)); \quad i = 1, ..6. \tag{15}$$

Finally, the new obstacle avoidance setpoint of the end-effector can be extracted according to the calculated setpoint of the second point of the cable ($X_{2e} c_i'$):

$$X_{2e} c_i' = (X_2 c_i' - X_2 c_i) + X_e; \quad i = 1 - 6. \tag{16}$$

This procedure can be done for each cable, and a new controlling signal can be calculated for each cable which is within the critical sphere of collision similar to the descriptions which is delivered for the end-effector obstacle avoidance. Summation of the controlling signals related to the cables which are within the critical zone of collision($\sum_{i=1}^{6} u_{2i^*}$) together with the controlling signal of the end-effector obstacle avoidance and the main controlling signal of the desired final setpoint is the final controlling signal which should be substituted in Eq. (7) in order to plan the optimal path. Thus, control signal is the summation of all of the signals related to the main control signal (related to the optimal path), obstacle avoidance related to the end effector and also obstacle avoidance related to all of the cables together. The proposed method is able to tune the gains related to each of these signals automatically depends on the level of collision risk which can be estimated using the distance of obstacle to each item. Summation of all of the mentioned signals will provide the safest path. Finally, it should be mentioned that the gain of derivative term in the linearized PID controller related to the obstacle avoidance needs to be set higher than the main setpoint since faster dynamic response is required for rounding the obstacle. The overall path planning of the optimal regulation of the cable robot in presence of obstacle can be seen in Fig. 3. Both of measurement and control are implemented on both of joints and end-effector. Rotation of the joints are measured using encoders and its linear states are controlled in the inner loop using PID each 0.01 s and the DOFs of the end-effector are measured using a hybrid sensors including of lasers and camera and their related nonlinear states are controlled in the outer loop using feedback linearization each 0.1 s. This method provides the required integration of feedback and feedforward terms of controlling signals to overcome the uncertainties and noises of an extreme nonlinear system like parallel robot of cable robot. Besides, the proposed method is able to round any predefined or nonpredefined obstacles if and only if the obstacle would be detected with a reasonable distance through the sensors and this distance is the radius of safety (RR) which is possible to be realized by the aid of employed sensors.

2.3. Adaptive controller and moving obstacle

The last step of controlling procedure is to add an adaptive controller to the designed controlling system to provide a good response for every environmental situation independent of the location and velocity of the obstacle. Since the end-effector movement is exponential as a result of using LQR optimizer, it has different velocities and accelerations in different points of its path and so a unique response of the end-efector is impossible due to a unique obstacle avoidance controlling input. Based on the circular motion dynamics we have $F = mv^2/r \Rightarrow r' = 2vv'm/F$. This fast decrease of radius provides a faster deviation from the main path in initial points of the end-effector movement and so less controlling force is required for the obstacles located in these points. Contrarily bigger controlling force is needed at the end of the path where the acceleration of the end-effector is low and so the produced radius of the circular motion decreases hardly. The required adaptive function should neutralize this effect throughout the path while preserving the stability of the end-effector using proper controlling gains which are dependent to the variable of the obstacle location. The following controlling gains are proposed for the cable robot which is evaluated based on the dynamics of the

https://doi.org/10.1017/S0263574714000691 Published online by Cambridge University Press

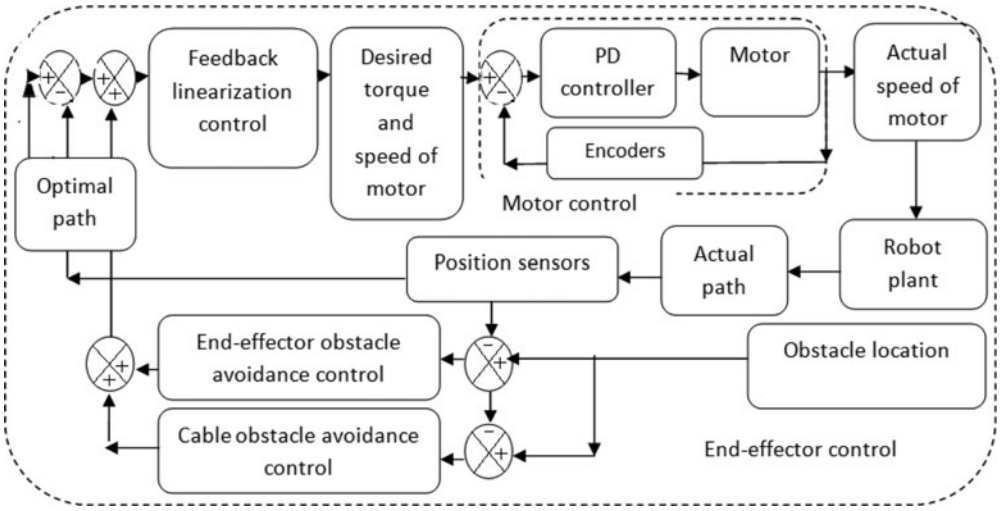

Fig. 3. Controlling procedure of optimal feedback linearization in presence of obstacle.

system:

$$v = k_1(d_{i-e}, d_{o-e})v_o + k_2(d_{o-e})v_e = \sqrt{d_{i-e}/4d_{o-e}}(RR - d_{o-e})/RR(v_o) + d_{o-e}/RR(v_e), \quad (17)$$

where k_1 and k_2 are the adaptive controlling gains of the main setpoint and obstacle avoidance setpoint respectively, is d_{i-e} the distance of initial point of the movement to the instantaneous position of the end-effector and d_{o-e} is the distance of the obstacle to the instantaneous position of the end-effector. These adaptive gains should provide a Gaussian shape controlling profile which could be produced practically by the aid of a DC motor and also should avoid any discontinuity and in stability of the end-effector. So the term $((r_o - d_{o-e})/RR)$ is used as the gain of obstacle avoidance to increase the obstacle avoidance controlling input continuously as the end-effector penetrates in the critical sphere which is defined around the obstacle. Also as it is mentioned, the more the obstacle is nearer to the initial point, required obstacle avoidance input is smaller. Since this increase should be proportional with the square value of the velocity ($F = mv^2/r$) and velocity is proportional linearly with the distance in LQR, the radical of the ratio of the end-effector distance to the initial point respect to its distance to the obstacle should be multiplied as the corrective gain of the obstacle avoidance ($\sqrt{d_{i-e}/4 \times d_{o-e}}$). In addition, the more the end-effector is close to the obstacle, the less control signal related to the main setpoint should be involved and that is why the gain of (d_{o-e}/r_o) is multiplied by the main controlling signal. Considering the fact that these gains are dependent to the relative distance and velocity of the end-effector respect to the obstacle (rather than the absolute values of them) independent of the location and velocity of the obstacle and end-effector, a unique Gaussian shape controlling signal will be produced which results in a unique obstacle avoidance response of the end-effector for stationary or moving obstacles in every environmental situation.

3. Simulation Study

3.1. Simple spatial case study

It is desired to find the optimal path of an under constrained spatial sample of cable robot with six DOFs and six actuators with specifications of Iran University of Science and Technology (IUST) cable robot of Table I. For all of the mentioned regulations, the accuracy controlling gains are set in a way that the end-effector reaches the target by about 10 s. By simple case here we mean that there is no obstacle within the path of the end-effector and the proposed obstacle avoidance strategy is not implemented for the optimal controller. The gain related to the altitude state of the end-effector (z) needs to be set higher than others in order to compensate the destructive effect of gravity. The end-effector is supposed to perform a regulation process by which the optimal path between these

https://doi.org/10.1017/S0263574714000691 Published online by Cambridge University Press

Table I. Characteristics of simulated of spatial cable robot of ICaSbot.

Name	Symbol	Value	Unit
Moment of inertia of the triangular end effector	I	$Ixx = Iyy = 0.0018; Izz = 0.0036; Iij = 0$	kg.m^2
Half of the base of triangular upper plate and end effector	a, b	0.59, 0.085	m
Error gain matrix	Q	diag[1]; $Q_Z = 50$	
Input gain matrix	R	diag[1]; $R_Z = 0.1$	
Radius of the motor	r	diag[0.015]	m
Damping coefficient	c	diag[0.01]	N.m/rad
Rotary inertia of the pulley	J	diag[0.0008]	kg.m^2
Mass of the robot	m	350	kg
Mass of the end effector	m	1.09	kg
Payload	m_l	2	kg

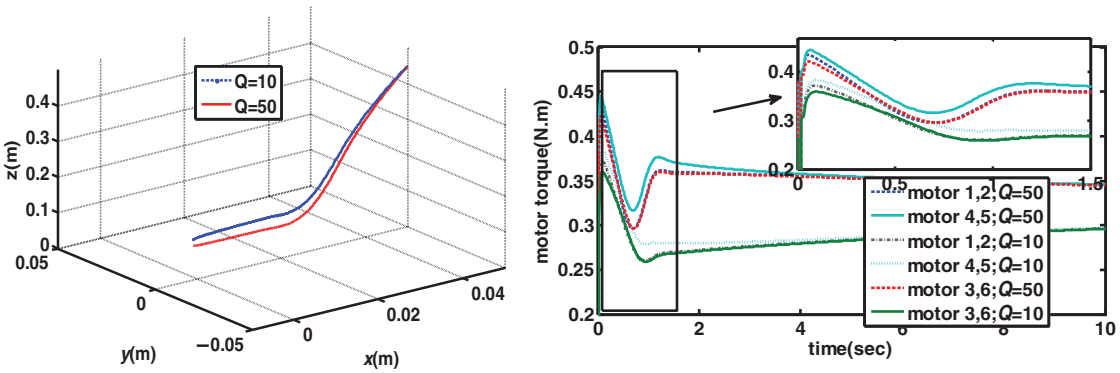

Fig. 4. Comparison of the optimal path for two systems (left) and its relative motor torque (right).

two initial and final points with initial and final velocity of zero could be extracted on-line:

$$X_0 = [0.05; 0; 0.45; 0; 0; 0]; \quad X_f = [0; 0; 0.1; 0; 0; 0]; \quad V_0 = [0; 0; 0]; \quad V_f = [0; 0; 0], \tag{18}$$

where X_0 is the initial position vector of the end-effector and X_f is its final destination vector. The payload of the end-effector is increased by 2 kg while the controller is designed for a 1 kg end-effector in order to examine the efficiency of the designed controller in neutralizing the effect of load uncertainty. Comparison of optimal path is performed for two systems with different error gain matrices. The first is $Q = \text{diag}[50]$ which is mentioned in Table I and the second is the system in which this gain is decreased to one tenth, i.e., $Q = \text{diag}[10]$. Also their relative motors' torque is shown in Fig. 4. The vectors of final point of each system are:

$$X_{f1} = (-0.0008, 0, 0.1408, 0, 0, 0); \quad X_{f2} = (-0.0007, 0, 0.1132, 0, 0, 0). \tag{19}$$

In a regulation process, the error of final point is important (since the trajectory is not predefined and is supposed to be extracted in and on-line and optimum way). It can be seen that the percentage of errors norm is about 0.011 for the system with bigger error gain matrix, while this value is about 0.04 for the latter case (about 10% improvement). It can be concluded that the controller with bigger error gain matrix improves its accuracy by increasing the required motors torque within its allowable bound and thus lets the system to have a higher payload. It can be seen that the error of the path's DOFs and its related motors' torque decrease exponentially as a result of usage of LQR optimizer tool. where Q_i is the component of the matrix Q related to state i and diag[j] is a diagonal matrix in which all of its diagonal elements are j. Comparison of the norm of velocity and acceleration of the end-effector during its optimal regulation is plotted in the Fig. 5. for the general case.

https://doi.org/10.1017/S0263574714000691 Published online by Cambridge University Press

Table II. Controlling parameters of the main controller and adaptive obstacle avoidance controller.

Name	Symbol	Value	Unit
Error gain matrix of main set point	Q	$Q_X = \text{diag}\,[1]; Q_Z = 50$	
Input gain matrix of main set point	R	$R_X = \text{diag}\,[1]; R_Z = 0.1$	
Error gain matrix of temporary set point	Q_o	$\text{diag}\,[10]$	
Input gain matrix of temporary set point	R_o	$\text{diag}\,[1]$	
Alpha	α	$r(t) = 50 \times d$	
Radius of safety sphere	RR	0.2	m
Radius of the obstacle	r_o	0.025	m

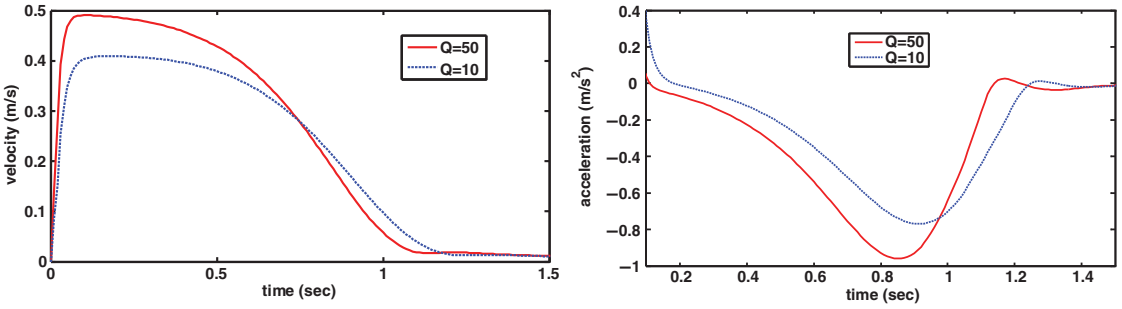

Fig. 5. Comparison of the end-effector velocity (left) and acceleration (right) for two different accuracy gains.

First of all, it can be seen that as it was expected the velocity and acceleration of the end-effector starts from zero and ends to zero also. Moreover, the exponential trend of LQR decrease is observable here too. The velocity and acceleration change during the time to realize the pole placement of the LQR. Finally as it is expected, the kinematic response of velocity and acceleration of the end-effector is bigger for the system in which the accuracy matrix is set higher to guide the end-effector toward its setpoint faster.

3.2. Spatial case considering adaptive obstacle avoidance

It is verified here firstly that if the obstacle avoidance can successfully bypass the local obstacle and secondly if the designed adaptive algorithm results in unique response of the end-effector movement independent of the obstacle location. To manage this verification, for end-effector obstacle avoidance a new scenario is considered here in which the obstacle is positioned in two different locations in the middle of the end-effector optimal path. Also, the test is performed for the case in which the obstacle is located at middle of the path of the first cable to verify the efficiency of the proposed algorithm for cable obstacle avoidance too. The initial and final vector points for end-effector obstacle avoidance and cable obstacle avoidance are as below:

$$\begin{array}{ll} \text{end}-\text{effector:} & X_0 = [0.05; 0; 0.45; 0; 0; 0]; \quad X_\text{f} = [-0.15; 0.2; 0.1; 0; 0; 0] \\ \text{cable:} & X_0 = [0.05; 0; 0.45; 0; 0; 0]; \quad X_\text{f} = [0; 0; 0.1; 0; 0; 0]. \end{array} \tag{20}$$

Control gains of the main set point and obstacle avoidance set point are presented in Table II. The location vectors of the obstacles are as below:

$$\begin{array}{ll} \text{end}-\text{effector:} & X_{O1} = [-0.087; 0.183; 0.05]; \quad X_{O2} = [0.009; 0.047; 0.339]\sqrt{2} \\ \text{cable:} & X_O = [0.1533; -0.375; 0.0934]. \end{array} \tag{21}$$

These points are the obstacle coordinated which can have any geometrical shape and size. According to the mentioned adaptive obstacle avoidance strategy, the optimal paths in which the obstacle is bypassed are obtained as Figs. 6(a)–6(d) for each case. Two first Figs are related to the optimal path of end-effector obstacle avoidance while the obstacle is placed in different places (in order to show the efficiency of the adaptive controller) and two last Figs are related to the paths of

https://doi.org/10.1017/S0263574714000691 Published online by Cambridge University Press

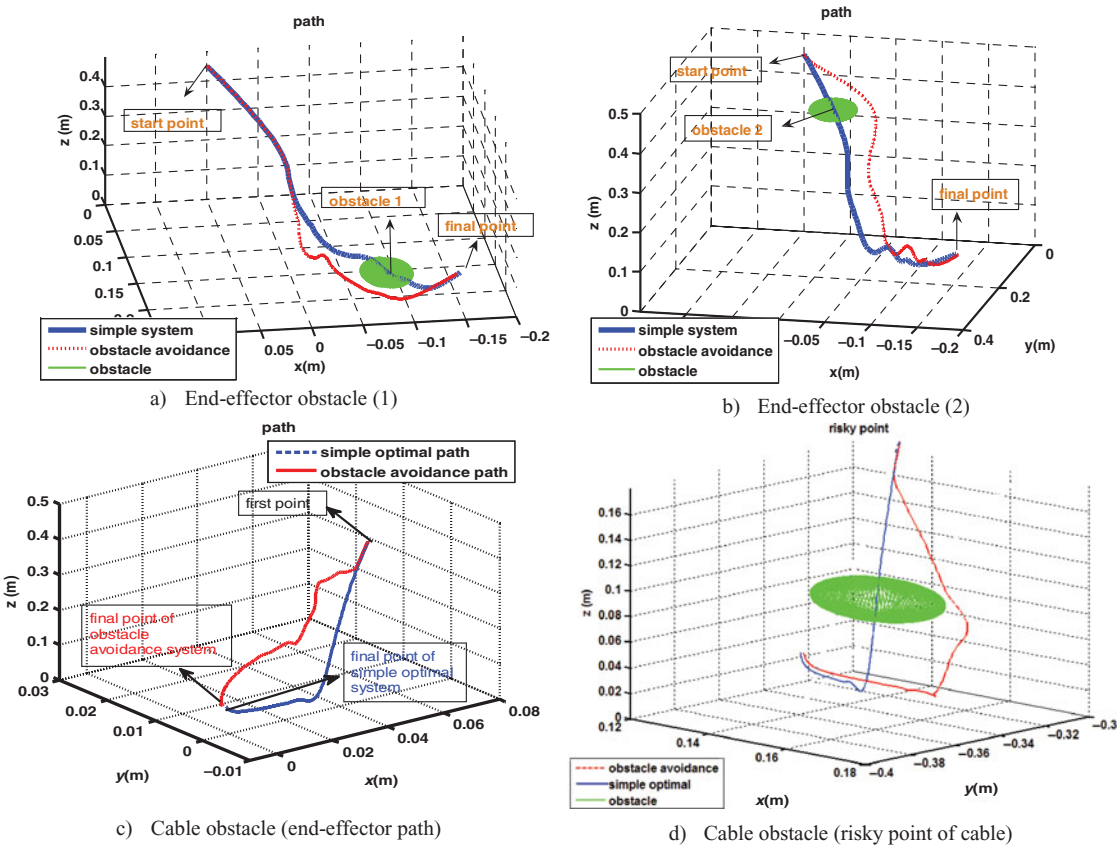

a) End-effector obstacle (1)

b) End-effector obstacle (2)

c) Cable obstacle (end-effector path)

d) Cable obstacle (risky point of cable)

Fig. 6. The effect of designed adaptive controller on obstacle avoidance system.

the end-effector and risky point of the cable for cable obstacle avoidance case (in order to show the efficiency of cable obstacle avoidance controller). It can be seen that for the both cases not only the obstacles are bypassed for all of the cases successfully, but also the safety distances are maintained roughly equal for all of these three different environmental situations which shows the efficiency of the designed adaptive controller. Also again the error of the final point of regulation process is roughly zero which shows the accuracy of the controller. It can be seen that the minimum distance for simple system is zero while this value is kept over about 3 cm for all of the systems equipped by obstacle avoidance. Moreover, based on the designed adaptive controller different motors torque is necessary in order to bypass these obstacles as it can be seen in the first 1.5 s of simulation for motor torques based on the (Fig. 7). For both cases of end-effector obstacle avoidance and cable obstacle avoidance, the designed controller exerts extra torque on the motors at the moment of approaching to the obstacles to bypass them. However, as it was expected this increase is more severe for the cable obstacle avoidance case since larger displacement at the end-effector position is required here to bypass the obstacle faced to the risky point of the cable. Besides, it can be seen that the peak of motors torque occurs in different stages according to the location of the obstacle.

However, the norm of these peaks is roughly the same which shows the efficiency of the designed adaptive controller.

3.3. Moving obstacle simulation

The obstacle can be also moving based on this strategy. In order to verify the efficiency of the proposed controller in this field, a moving obstacle which has a time function of Eq. (22) is placed within the way of optimal path of Eq. (18).

$$X_o = [-0.032(t/0.5); -0.11(t/0.5); 0.22(t/0.5)], \tag{22}$$

https://doi.org/10.1017/S0263574714000691 Published online by Cambridge University Press

Table III. Controlling parameters of the main controller and obstacle avoidance controller for moving obstacle.

Name	Symbol	Value	Unit
Error gain matrix of main set point	Q	$Q_X = \text{diag}\,[1]; Q_Z = 200;$ $Q_{X'} = \text{diag}\,[0.11]; Q_{Z'} = 20$	
Input gain matrix of main set point	R	diag[1];	
Error gain matrix of temporary set point	Q_o	$Q_X = \text{diag}\,[10]; Q_{X'} = \text{diag}\,[30]$	
Input gain matrix of temporary set point	R_o	$diag[1]$	
Alpha	α	$r(t) = 1 \times d$	
Radius of safety sphere	RR	0.25	m
Radius of the obstacle	r_o	0.025	m

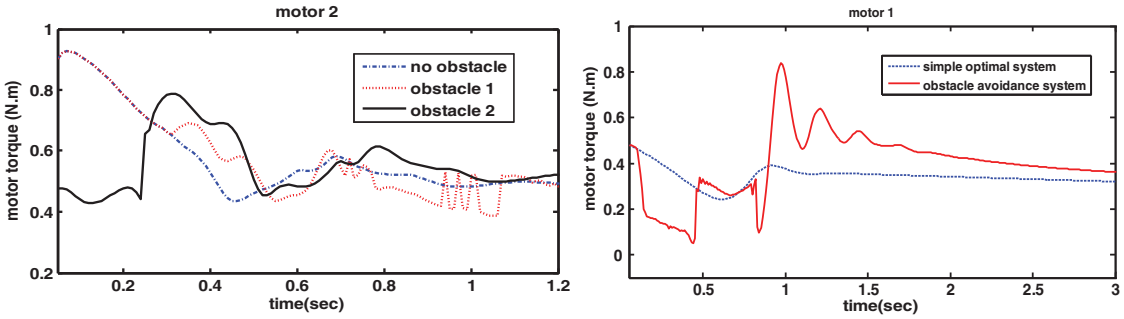

Fig. 7. Comparison of motor torque for different locations of end-effector obstacle (left) cable obstacle (right).

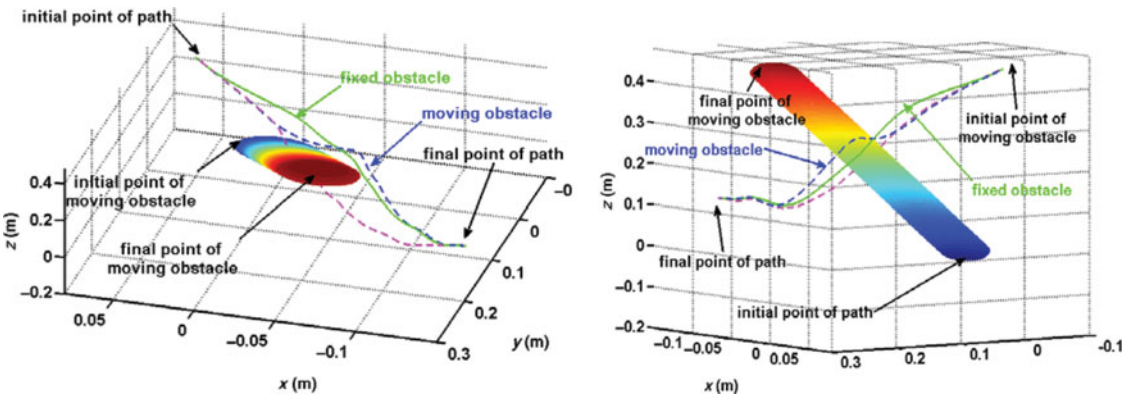

Fig. 8. Comparison of the optimal path and efficiency of obstacle avoidance (left). The moving obstacle is perpendicular to the motion of the end-effector (right).

where t is time. Required obstacle avoidance specifications are set as Table III to enable the robot to bypass this moving obstacle. Here, the direction of moving the obstacle is roughly perpendicular to the direction of the end-effector to show the efficiency of the proposed method for the worst case. The optimal path for the systems which are equipped by the obstacle avoidance with moving and fixed obstacles and its comparison with the simple system are shown in the Fig. 8.

It can be seen that the proposed controlling scheme has successfully passed the moving and fixed obstacles with roughly similar minimum critical distance. Comparison of the required motors torque near the moment of bypassing the obstacle is depicted in Fig. 9(right) and their related critical distances can be seen in Fig. 9(left).

It is observable that the required increase in the torque for the moving obstacle case are more than fixed one since the end-effector has a less time to round the moving obstacle. The optimal path of fixed obstacle has been deviated sooner than the moving case since the obstacle is closer to the end-effector at the initial time and the end-effector enters the critical sphere sooner.

https://doi.org/10.1017/S0263574714000691 Published online by Cambridge University Press

Table IV. Motor characteristics and controlling gains of simulated full load spatial cable robot.

Name	Symbol	Value	Unit
Maximum allowable error bounds of tracking	R_e	0.01	m
Free running angular velocity of the motors	ω_n	286.5	rpm
Error gain matrix	Q	$Q_X = 25; Q_z = 250$ $Q_{X'} = 10; Q_{z'} = 100$	
Input gain matrix	R	diag [0.1]	
Stall torque of the motors	τ_s	0.75	N.m

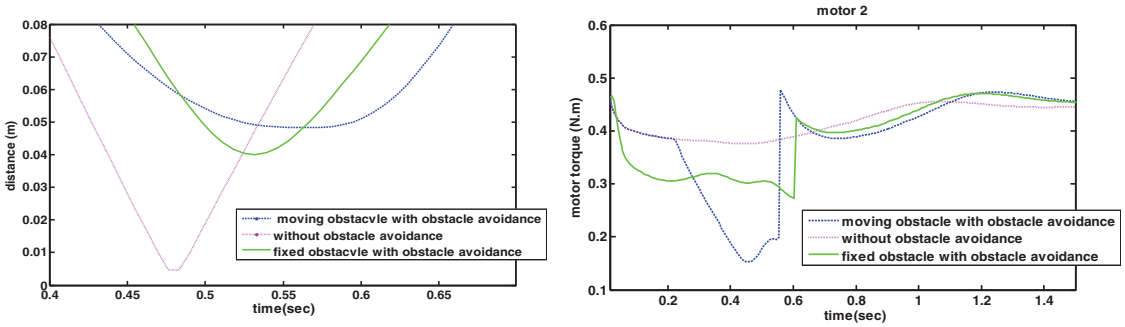

Fig. 9. Comparison of distance to obstacle (left). Required motor torque for fixed and moving obstacles (right).

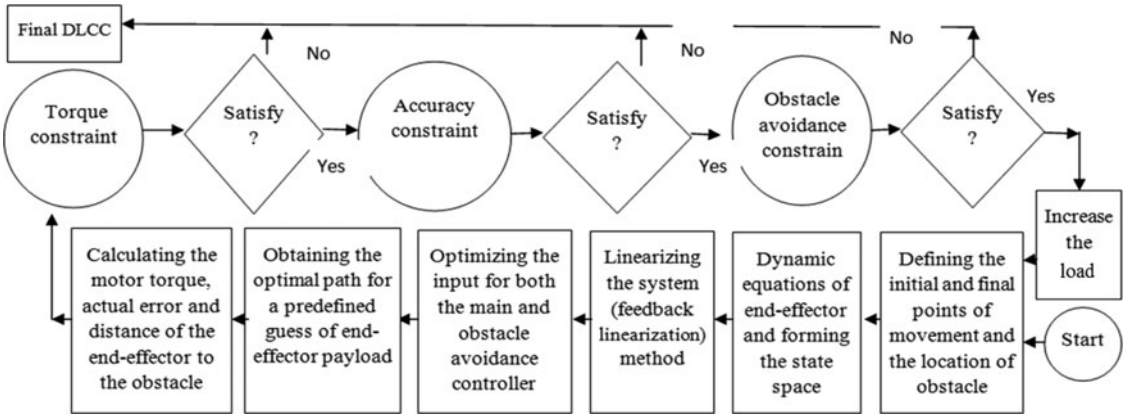

Fig. 10. Algorithm of defining the optimal closed loop DLCC of a cable robot.

4. DLCC Formulation and Simulation

DLCC is defined as the maximum load which the end-effector can carry along a path with a specific velocity while all of the constraints could be satisfied simultaneously.

In this paper, the main constraints are accuracy of the end-effector, torque saturation of the motors and obstacle avoidance. Iterative method based on Fig. 10 is employed to obtain the optimal DLCC of a cable robot in presence of obstacle in a closed loop way.[14] Here, the load increases for the optimized system in each iteration and all of the constraints are checked to be satisfied. As soon as the first violation occurs for any constraint the last load is defined as the maximum DLCC. Maximum DLCC based on this method occurs when both of torque and error bounds saturate simultaneously for the optimized system and the condition of obstacle avoidance is satisfied as well.

4.1. Simple spatial case

This algorithm is implemented for the manufactured spatial cable robot of ICaSbot. The initial and final points are the same as Eq. (18) and the motor characteristics and the chosen optimal controlling gains (to achieve the highest DLCC) are according to Table IV:

https://doi.org/10.1017/S0263574714000691 Published online by Cambridge University Press

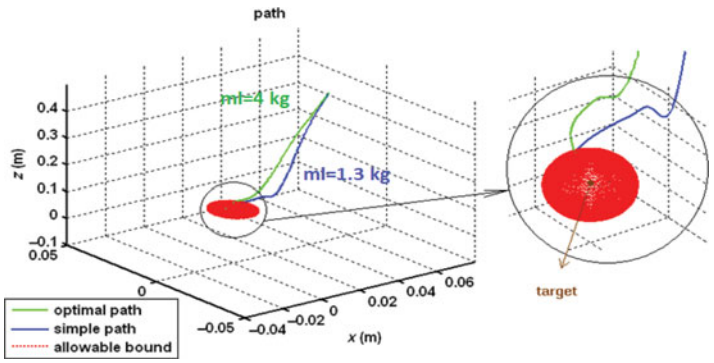

Fig. 11. Optimal trajectory with respect to allowable error zone.

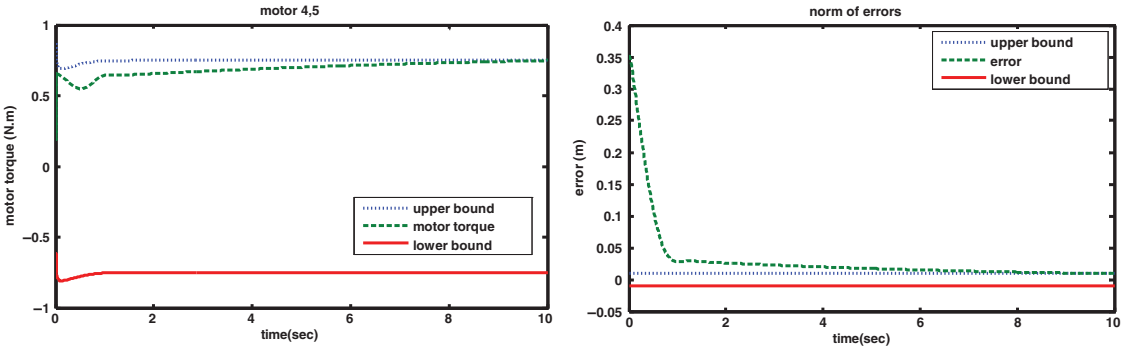

Fig. 12. Motors torque saturation (left) and error saturation profiles (right).

Maximum payload of 4kg is the consequence of LQR usage and simultaneous saturation of error and torque by the aid of chosen controlling gains of Table IV. The optimal trajectory of the end-effector with respect to the sphere which represents the allowable error bound is shown in Fig. 11 (The final points are tangent to the sphere). Moreover, saturation profile of the motors torque and error are shown in Fig. 12. The first motor saturation occurs for the motors 4 and 5. As it can be seen the upper bound is a function of actual angular velocity of the motor and changes a little bit during the time.[14]

This payload is considerably more than the DLCC of the nonoptimized system for which the gains are not optimized (the DLCC of nonoptimized system is 1.3 kg). For this system, the error constraint saturates before that any saturation occurs for the motors torque. Thus, it can be concluded that the optimized controlling gains of LQR provides the maximum result for DLCC. The speed of movement is not important here since the time is not included in the objective functions and the proposed method optimizes the DLCC.

4.2. Spatial case considering obstacle avoidance

Motor characteristics and controlling gains are based on Table V. The optimal path for the system which is equipped by an obstacle avoidance controller and the one which is working without this feature are compared in the Fig. 13. Using the DLCC algorithm in this case, results in 2.5 kg load capacity for which the obstacle is placed in the middle of the optimal path:

$$X_O = [0.02177; 0; 0.1558]. \tag{23}$$

Torque and error saturation for this optimal path which bypasses the obstacle is shown in Fig. 14. Considering the sudden increase of motors torque at the moment of approaching to the obstacle, the first saturations occur for second, fourth, and fifth motors torque simultaneously.

As it was expected, the sudden increase in the motors torque at the moment of passing the obstacle causes sooner saturation in motors with a payload of 2.5 kg which is 1.5 kg less than the one which was calculated for the simple case but the obstacle is successfully bypassed here. As it was

https://doi.org/10.1017/S0263574714000691 Published online by Cambridge University Press

Table V. Motor characteristics and controlling gains of obstacle avoidance controller for full load end effector.

Name	Symbol	Value	Unit
Error gain matrix for the main set point	Q	$Q_X = 10; Q_z = 100$ $Q_{X'} = 5; Q_{z'} = 55$	
Input gain matrix for the main set point	R_1	diag[0.1]	
Error gain matrix for the temporary set point	Q_O	$Q_X = 50$ $Q_{X'} = 80$	
Input gain matrix for the temporary set point	R_O	diag [1]	
Alpha	α	$r(t) = 55 \times d$	
Radius of safety sphere	R	0.15	m

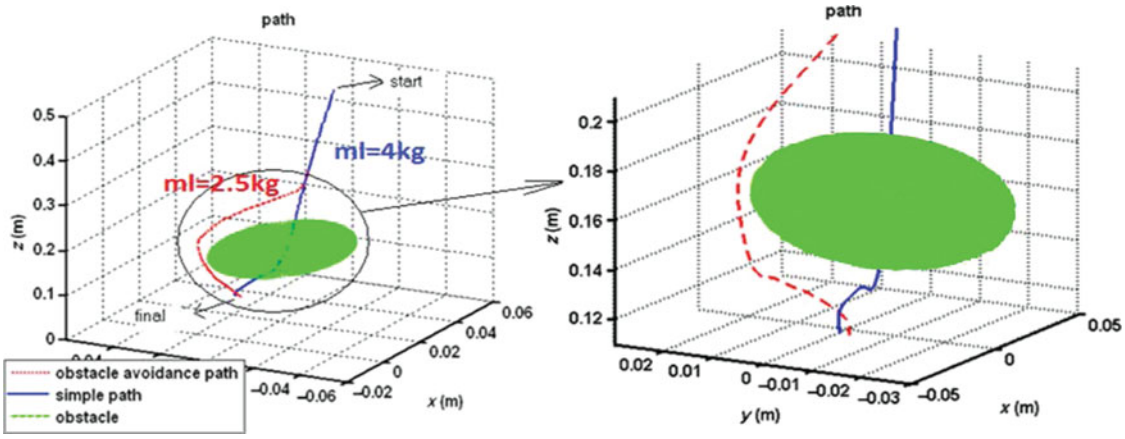

Fig. 13. Comparison of the optimal path of full-load end-effector for simple and obstacle avoidance controller.

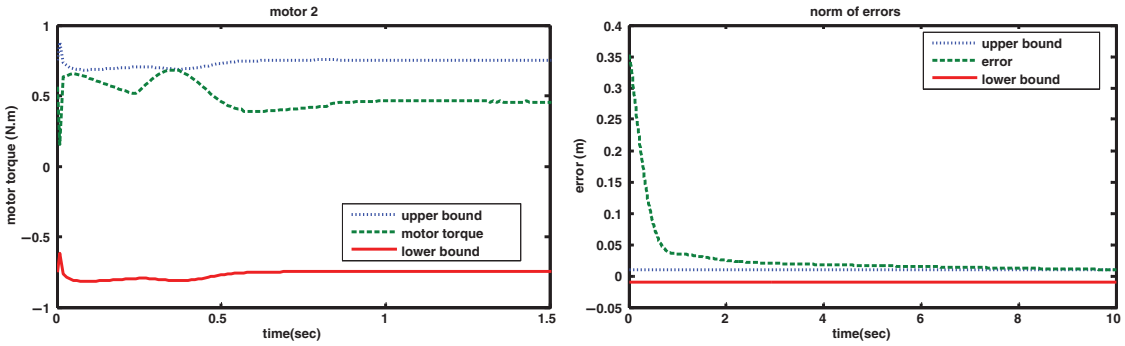

Fig. 14. Motors torque saturation (left) and its relative error saturation (right).

expected, the DLCC is decreased for the obstacle avoidance system since the required torque to bypass the obstacle has a peak for this moment. However, considering the fact that both of the main and obstacle avoidance regulations are optimized, this DLCC value for obstacle avoidance case is again the maximum between other possible paths.

5. Experimental Verification

To verify the proposed optimal regulation of cable robot, and efficiency of the explained obstacle avoidance strategy, experimental tests are conducted on the designed and manufactured cable robot of IUST called ICaSbot (Fig. 15).

This cable robot is an under constrained cable robot supporting six DOFs using six actuating cables and six DC motors.[16] In order to plan the optimal path and control the end-effector to bypass the obstacle, the mentioned optimal feedback linearization is employed to control the end-effector

https://doi.org/10.1017/S0263574714000691 Published online by Cambridge University Press

Table VI. Characteristics of the used DC motors and encoders.

Motor's specification	Value	Encoder's specification	Value
Mark	Retarding Gear Motor	Mark	Autonics
Model	1.61.070.304 Buhler	Model	E50S8–600–3-T-24
Reference voltage	12 v	Resolution	600
No load speed	150 rpm	Output phase	A, B, Z
Stall torque	1.7 N.m	Control Output	Totem pole
No load current	0.3 A	Power supply	12–24 v
Stall current	1.2 A	Max allowable revolution	5000 rpm
Reduction ratio	1:175		
Weight	220 g		

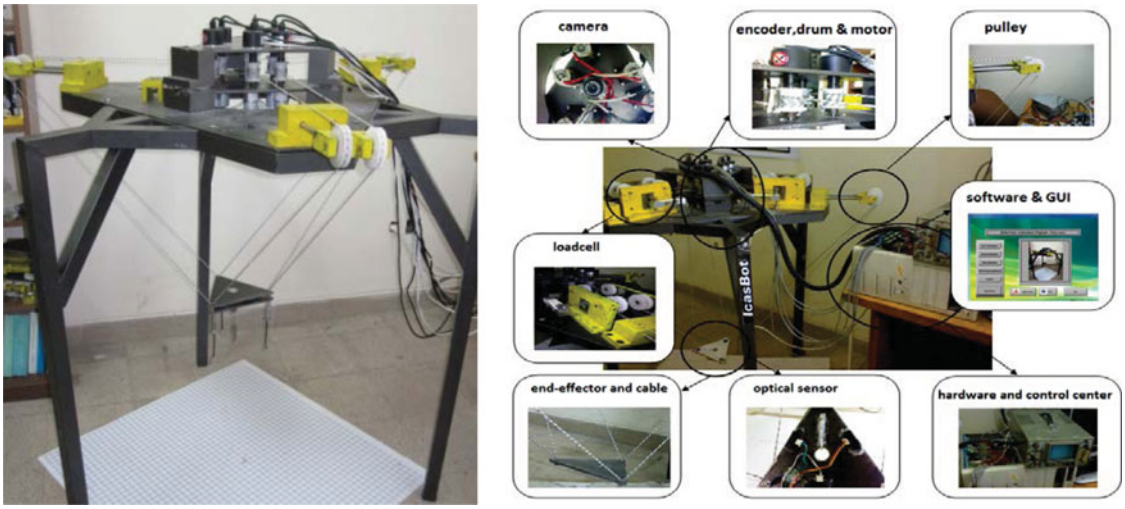

Fig. 15. Overall scheme of ICaSbot (left). Its components and control center (right).

(Fig. 3). Also PWM method is used to control the motors based on feed forward terms of inverse dynamics and feedback terms of PD controller. It is tried to control both of torque and speed of DC motors by the aid of PWM method to satisfy both of kinematics and kinetics which are necessary to provide our regulation process. This importance is realized here by the aid of extracting the characteristic curve of the motor by which the relation between three parameters of torque, speed and PWM can be obtained. Characteristics of the used DC motors and encoders are as Table VI.

Thus again based on Fig. 3 two sequential controlling loop is employed to conduct the experimental tests. In the inner loop, the linear system of motors are controlled using linear PID controller each 0.01 s while the nonlinear end-effector is also controlled in the outer loop using a nonlinear strategy of feedback linearization each 0.1 s. Among the nonlinear methods, feedback linearization is the most applicable one since the least calculation and processing is required and it can be implemented experimentally in an on-line way. That is why a fast obstacle avoidance method is required here to follow this fine sample rate process. Six loadcells are used to monitor the actual kinetic of cables' tension and six 600 pulse/round encoders are installed to estimate the actual angular velocity of the motors. Since, the measurement of all of the states of a six DOFs cable suspended robot is somehow complicated, a combination of laser and camera is employed in order to record and feedback the actual position and orientation of the end-effector. Three lasers are responsible of evaluating the altitude of the end-effector together with its rotational movement, while the camera which is installed at the top of the structure measures its planar movement by the aid of an online feedback of its altitude received by the lasers to satisfy its perspective formulations. Lasers and camera cover the measurement process with 0.1 sec sample rate which is required for outer loop feedback process of the controller. Finally, the states related to the velocity of the DOFs are estimated using numerical differentiation in the software.

https://doi.org/10.1017/S0263574714000691 Published online by Cambridge University Press

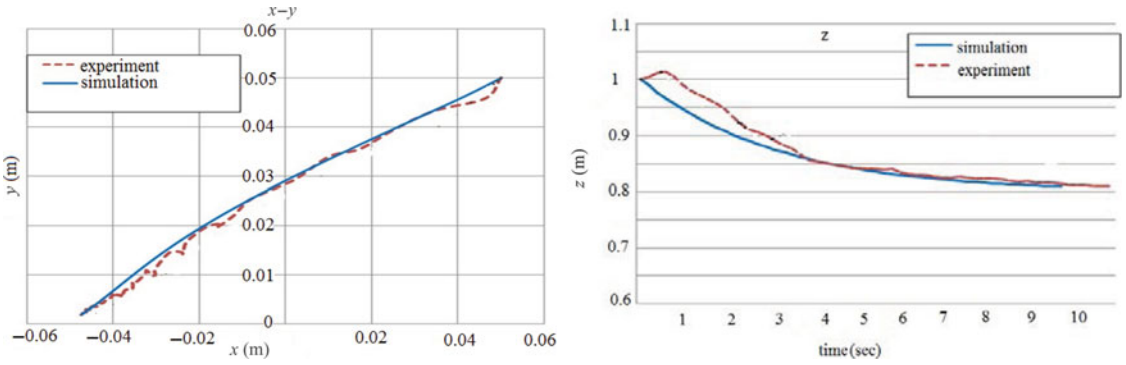

Fig. 16. Comparison of optimal path in regulation process for simulation and experimental test.

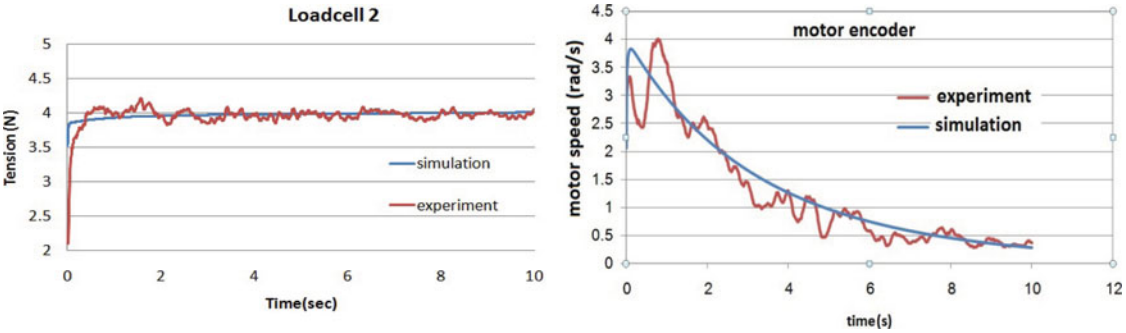

Fig. 17. Comparison of cable tension for simulation and experiment (left) and motor speed (right).

5.1. Simple regulation case considering load uncertainty

In this section, it is proved that the robot is able to perform an optimal regulation movement from one specific point to other specific goal. For this movement a payload equal to 0.8 kg is placed on the end-effector in order to investigate the ability of the designed controller to neutralize the destructive effects of load uncertainty. Controlling specifications of the robot is similar to Table I and initial and final points of the robot are as below for 10 s motion:

$$X_0 : (0.05, 0.05, 1); \quad X_f : (-0.05, 0, 0.8). \tag{24}$$

Three-dimensional (3-D) motion of the end-effector can be seen in Fig. 19(left). Comparison of optimal path between simulation and experiment is as Fig. 16. Good compatibility and exponential decrease proves the efficiency of the proposed regulation process.

The same comparison is done for angular velocity of the motors and load cell (Fig. 17). Similar to the profile of DOFs, the angular velocity of the motors decreases exponentially during the time. The Loadcell increases during the time since the motion is upward and a payload is placed on the end-effector. There are also some vibrating behavior in the profile of experimental results around the mean value of simulation profiles which is the result of existence of clearance in the motors, cables vibration, structural flexibilities and other unmodeled uncertainties.

5.2. Obstacle avoidance case

Eventually, to investigate the obstacle avoidance capability of the proposed method, the optimal path between the same points of Eq. (24) is extracted experimentally by the aid of ICaSbot while a stationary obstacle is placed within its path with radius of 2 cm:

$$X_o = [0.01; 0.036; 0.927]; \quad r_o = 2\text{cm}. \tag{25}$$

Required controlling specifications are similar to the Table II. Comparison of the optimal path in presence of obstacle between simulation and experimental results is shown in Fig. 18:

https://doi.org/10.1017/S0263574714000691 Published online by Cambridge University Press

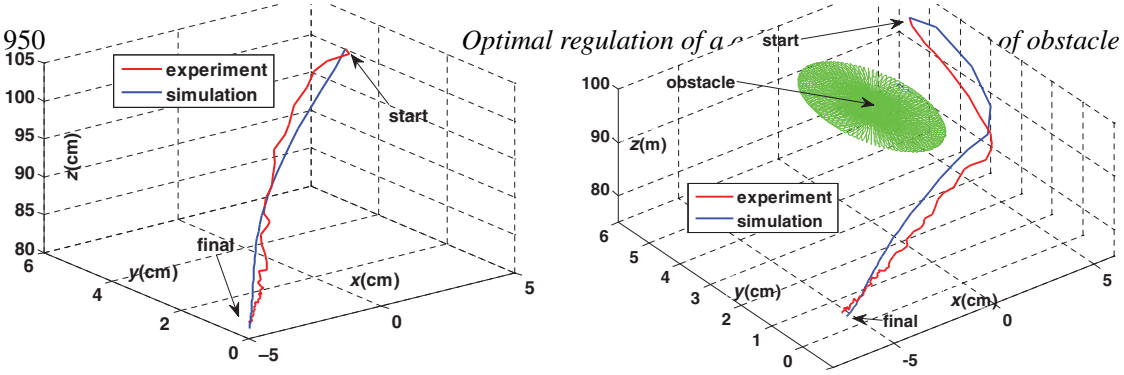

Fig. 18. Comparison of optimal path in presence of obstacle for simulation and experimental test.

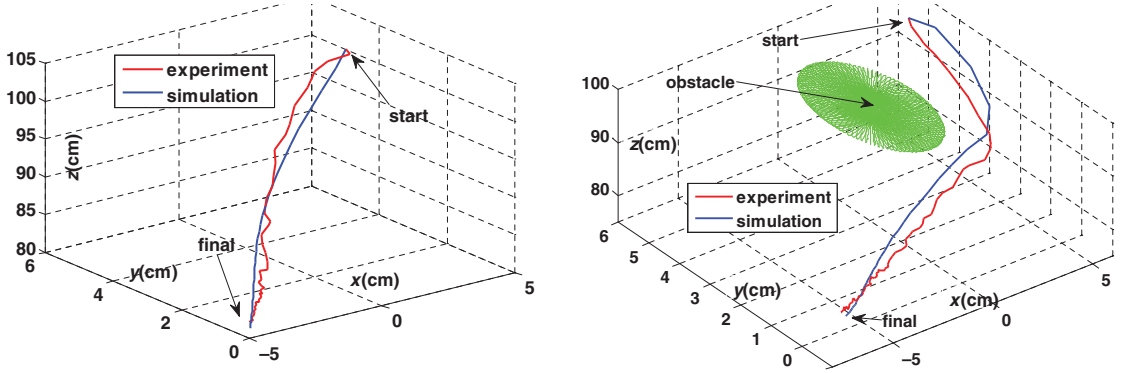

Fig. 19. Comparison of 3-D motion of the end-effector, simple (left), with obstacle (right).

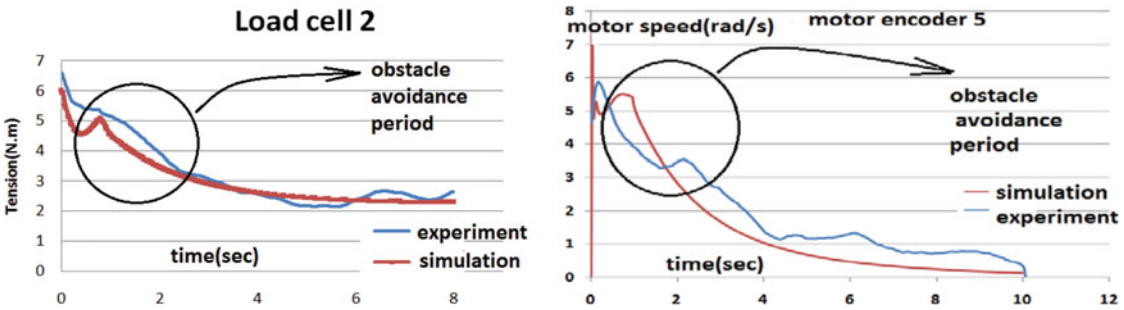

Fig. 20. Comparison of cable tension for simulation and experiment (left) and motor speed (right).

However it seems that collision occurs in *x*-*y* plane, considering isometric and 3-D motion of the end-effector it can be seen in Fig. 19(right) that the obstacle is by passed successfully with a good safety margin for both the simulation and experiment which shows the efficiency of the proposed obstacle avoidance strategy:

It can be seen that the proposed protocol of obstacle avoidance is fast enough to be used experimentally in an on line way to round an obstacle as a result of linearizing the system and using linear objective function. Here, again it is supposed that the obstacle avoidance should bypass a sphere which encompasses the obstacle with its complicated geometrical shape which is safer. However, following the maximum DLCC strategy explained in section four results in the maximum allowable load. Comparison of cable tension and also angular velocity of the motor is shown in Fig. 20. For both profiles, there is a zone in which a little peak occurs in the profiles of kinetics results (required change in cable tension) and kinematics results (resultant change in motor speed) which is related to obstacle avoidance period. Although there is a delay for this deviation related to obstacle avoidance between simulation and experiment which is the result of friction and inertia of the motors. Moreover, considering the fact that the presented obstacle avoidance is local and on-line, it is obvious that the controlling commands related to bypassing the obstacle switches based on the information received from the sensors and a little oscillatory response is unavoidable.

https://doi.org/10.1017/S0263574714000691 Published online by Cambridge University Press

But as it can be seen, the proper controlling parameters and LQR help us to decrease this vibration and as it can be seen the response is acceptable. However, the same pattern of profile trends proves the efficiency and validity of the proposed obstacle avoidance strategy.

6. Conclusion

Optimal path with the maximum DLCC was obtained for the closed loop system of cable suspended robot between two predefined points in presence of obstacle. This goal was achieved by proposing a new method of optimal regulation for non linear systems which is based on optimal feedback linearization approach. It was shown that not only this movement is robust in presence of uncertainties, but also is able to bypass local and moving obstacles. It was stated that contrary to previous works, both of proposed optimal regulation and obstacle avoidance methodology have the privilege of linearized nature and so fast calculation process makes it suitable to be practically applicable in on-line and real time experimental manipulations. It was seen that based on this proposed optimal regulation, all of the dynamics responses of the end-effector changes exponential as a result of LQR usage. It was shown that the controller with bigger error gain needs higher motor torque and faster response which provides better accuracy (about 10% improvement) through the planned path and vice versa. Local obstacle avoidance was considered in this paper by designing an adaptive obstacle avoidance controller which helps the end-effector and also the cables to bypass a local and moving obstacle in every environmental situation in an on-line way and with the optimal energy. It was seen that adding the obstacle avoidance controller to the system causes the motors torque to be increased at the moment of passing the obstacle by about 10% while this amount is even bigger for cable obstacle avoidance case for which a larger displacement is required for the end-effector. Maximum DLCC of the system was finally calculated analytically for the obtained optimal path by the aid of an iterative algorithm considering motors torque, accuracy and obstacle avoidance constraints. It was shown that using LQR, maximizes this parameter more than 50% compared to the simple systems. Moreover it was seen that higher torque which is necessary for bypassing the obstacle compared to the simple case, causes the end-effector to have a lower payload (about 30% decrease). All of the results were validated by using some experimental studies. The acceptable compatibility of simulation and experiment proved the correctness of regulation process and confirmed the exponential behavior of the end-effector movement as the result of using LQR. The vibrating nature of experimental profiles is related to flexibilities and other unmodeled uncertainties. It was shown that the obstacle can also be bypassed experimentally by the aid of the proposed obstacle avoidance controller which produces a little, inevitable deviation in the profile of dynamic response of the robot during the obstacle avoidance period.

References

1. M. H. Korayem, Kh. Najafi and M. Bamdad, "Synthesis of cable driven robots' dynamic motion with maximum load carrying capacities: Iterative linear programming approach," *Trans. B: Mech. Eng.* [Sharif University of Technology], **17**(3), 229–239 (Jun. 2010)
2. M. H. Korayem, M. Bamdad and S. Bayat, "Optimal Trajectory Planning with Dynamic Load Carrying Capacity of Cable-suspended Manipulator," *IEEE International Symposium Mechatronics and its Applications (ISMA)* (2009) pp 1–6.
3. Y. Li and X. Chen, "Mobile Robot Navigation Using Particle Swarm Optimization and Adaptive NN," *Lecture Notes in Computer Science*, 3612 (PART III) (2005) pp. 628–631.
4. Sh. Fang, D. Franitza, M. Torlo, F. Bekes and M. Hiller, "Motion control of a tendon-based parallel manipulator using optimal tension distribution," *IEEE/ASME Trans. Mechatronics* **9**(3), (Sept. 2004) pp. 561–568.
5. P. Gholami, M. Aref and H. D. Taghirad, "On the Control of the KNTU CDRPM: A Cable Driven Redundant Parallel Manipulator," *IEEE/RSJ International Conference on Intelligent Robots and Systems, Acropolis Convention Center*, Nice, France (Sep. 22–26, 2008).
6. Y. Zhang, S. K. Agrawal, P. R. Hemanshu and M. J. Piovoso, "Optimal Control using State Dependent Riccati Equation (SDRE) for a Flexible Cable Transporter System with Arbitrarily Varying Lengths," *Proceedings of the 2005 IEEE Conference on Control Applications*, Canada (Aug. 28–31, 2005).
7. M. H. Korayem, V. Azimi, A. Nikoobin and Z. Boroujeni, "Maximum load-carrying capacity of autonomous mobile manipulator in an environment with obstacle considering tip over stability," *J. Adv. Manuf. Technol.* **46**(5–8), 811–829 (2010).

https://doi.org/10.1017/S0263574714000691 Published online by Cambridge University Press

8. Y. Koren and J. Borenstein, "Potential Field Methods and Their Inherent Limitations for Mobile Robot Navigation," *Proceedings of the International Conference on Robotics and Automation* (1999) pp.1398–1404.
9. D. H. Kim and S. Shin, "Local path planning using a new artificial potential function composition and its analytical design guidelines," *Adv. Robot.* **20**(1), 115–135 (2006)
10. D. Yang and S. Hong, "A roadmap construction algorithm for mobile robot path planning using skeleton maps," *Adv. Robot.* **21**(1–2), 51–63 (2007).
11. T. Kubota, H. Hashimoto and F. Harashima, "Path searching for a mobile robot by local planning," *Adv. Robot.* **5**(4), 397–410 (1991).
12. C. Forest, D. Frakes and W. Singhose, "Input-Shaped Control of Gantry Cranes: Simulation and Curriculum Development," *ASME DETC 18th Biennial Conference on Mechanical Vibration and Noise*, Pittsburgh, PA (2001).
13. A. B. Alp, Cable Suspended Parallel Robots, *MSc. Thesis* (Mechanical Engineering Department, University of Delaware, 2001)
14. M. H. Korayem and H. Tourajizadeh, "Maximum DLCC of spatial cable robot for a predefined trajectory within the workspace using closed loop optimal control approach," *J. Intell. Robot. Syst.* **63**(1), 75–99 (2011).
15. F. Lin, *Robust Control Design an Optimal Control Approach*, (Wayne State University, USA and Tongji University, China, Published by John Wiley & Sons Ltd, England, 2007).
16. M. H. Korayem, M. Bamdad, H. Tourajizadeh, H. Shafiee, R. M. Zehtab and A. Iranpour, "Development of ICaSbot a cable suspended robot with 6 DOFs," *Arab. J. Sci. Eng.* **38**, 1131–1149 (2013).

https://doi.org/10.1017/S0263574714000691 Published online by Cambridge University Press